

Article

Measurement and Analysis of Light Leakage in Plastic Optical Fiber Daylighting System

Kunhao Liu ¹, Lianglin Zou ¹, Yuanlong Li ¹, Kai Wang ¹, Haiyu Wang ¹ and Jifeng Song ^{2,*}¹ School of New Energy, North China Electric Power University, Beijing 102206, China² Institute of Energy Power Innovation, North China Electric Power University, Beijing 102206, China

* Correspondence: solarsjf@163.com

Abstract: The daylighting systems via polymethylmethacrylate (PMMA) plastic optical fibers have obvious cost advantages and have been widely studied. However, there is light leakage when PMMA optical fibers transmit concentrated sunlight, resulting in a transmission efficiency lower than the theoretical value. This research aims to quantitatively study the light leakage effect of PMMA optical fibers. Concentrated sunlight was used as the sunlight source instead of a monochromatic laser. An adjustable diaphragm was used to adjust the angle of the incident light, and the infrared filter and heat-absorbing glass were used to solve the overheating problem of PMMA fibers. The results show that when the incident angle is greater than 13°, the relative transmission efficiency of the fibers drops rapidly, which means that the light leakage deteriorates. The data also show that the angle of the output beam of PMMA optical fibers is $\pm 30^\circ$, which is independent of the angle of the incident beam. Based on this conclusion, a PMMA optical fiber daylighting system with an incident angle of 13° was developed, which has higher transmission efficiency than previously developed systems. This study indicates that the angle effect of light leakage should be considered in the design of a plastic optical fiber daylighting system.

Keywords: light leakage; daylighting system; plastic optical fibers; light distribution



check for updates

Citation: Liu, K.; Zou, L.; Li, Y.;

Wang, K.; Wang, H.; Song, J.

Measurement and Analysis of Light Leakage in Plastic Optical Fiber Daylighting System. *Sustainability* **2023**, *15*, 3155. <https://doi.org/10.3390/su15043155>

Academic Editor: Ramchandra Ponde

Received: 14 November 2022

Revised: 2 February 2023

Accepted: 7 February 2023

Published: 9 February 2023



Copyright: © 2023 by the authors. Licensee MDPI, Basel, Switzerland. This article is an open access article distributed under the terms and conditions of the Creative Commons Attribution (CC BY) license (<https://creativecommons.org/licenses/by/4.0/>).

1. Introduction

As a ubiquitous renewable energy source, solar energy is very popular in the field of low-carbon buildings. Lighting is an important part of building energy consumption [1,2]. For commercial buildings, lighting electricity consumption accounts for around 20–30% of the total building energy consumption [3,4]. Bringing daylight into the room can reduce electric lighting by 50–80% [5]. At the same time, because the output spectrum of daylighting systems is similar to the natural spectrum [6], daylighting can improve human visual comfort, allow people to relax, provide positive psychological suggestions, and even cure diseases [7,8]. Using as much natural light as possible in buildings is an efficient and easy low-carbon option [9–11].

The optical fiber daylighting system transmits outdoor sunlight into the interior for lighting [12,13]. It uses a sun tracking and a focusing technique [14]. Fiber daylighting systems can concentrate sunlight to a high level and then transmit it through flexible optical fibers into the interior for lighting, allowing for natural light within buildings [15]. This technology breaks through the limitations of the building structure and can transmit flexibly [16]. It delivers natural light remotely to shaded rooms, basements, etc. [17]. It can also be used for decorative lighting at the bottom of swimming pools, museums, ammunition depots, and other special places where fire and electricity are strictly prevented [18]. Due to these advantages, fiber optic daylighting systems have received significant attention in recent years [19].

In general, a fiber daylighting system consists of three parts: a sun tracking system, a focusing system, and optical fibers [20]. The focusing system focuses the sunlight onto the

end face of the fiber [21,22], usually choosing parabolic mirrors [23] or lenses [24]. Silica fibers and polymethylmethacrylate (PMMA) plastic fibers are both used to transmit focused sunlight. The high cost of using silica fibers as a transmission medium makes it difficult to scale up [25]. The diameter of the focused spot generated by the lens is generally 0.5–2 mm. Transmission of this size of the flux requires a beam composed of hundreds of silica fibers with a diameter of 100 μm , and the cost is difficult to reduce [26]. However, PMMA plastic fibers perfectly avoid this cost bottleneck [27]. The typical diameter of PMMA plastic fiber is 0.5–3 mm, and the acceptance angle can reach 30° , which can be perfectly coupled with the concentrating flux of the lens [28]. In the meantime, the cost of plastic optical fiber is only one-thousandth of that of the quartz fiber bundle with the same diameter [29]. Due to the high transmittance and low cost, plastic optical fibers show high potential in daylighting systems [30]. Ullah and Shin [31] combined plastic fibers with silica fibers for daylighting in multi-story buildings. Lv et al. [32] developed a highly flexible system via optical fibers. A new fluctuation control method in an optical fiber daylighting system was studied by Barbón et al. [33]. Song et al. [34] designed a plastic fiber daylighting system with large Fresnel lenses. Laila et al. [35] designed a parabolic solar daylighting system based on fiber optic wires. Savović et al. [36,37] investigated the performance properties of POFs employed as a part of a traffic light system and the temperature dependence of mode coupling in low-NA POFs.

Han et al. [38] found that the intensity distribution of the output illuminance in PMMA optical fiber daylighting systems is significantly inhomogeneous. There is a nonlinear relationship between the transmittance of optical fiber and the incident angle. When the incident angle exceeds 15° , the transmittance of the optical fiber decreases rapidly [39]. This is due to numerous causes of loss, the most significant of which is light leakage [40]. The interface between the cladding and the fiber core is slightly damaged, which destroys the total internal reflection condition and causes light leakage. Mildner and Chen [41] used a model with a constant absorption loss for each reflection at the core-cladding interface to study the light leakage. It was only applied in special situations with narrow-spectrum and low numerical aperture fibers. Liang [42] and Nakamura [43] demonstrated that this model could not be applied to fibers with wide-spectrum and high numerical aperture. Dugas et al. [44] suggested that light leakage is due to the large amount of reflection of incident light at the core-cladding interface. Feuermann [45] analyzed the angle of the incident, the optical properties of the core and cladding, and the fiber length on light leakage.

Clarifying the details of light leakage will help in the design of optical fiber daylighting systems. There are very few studies on the relationship between the transmittance and the angle of incident of large-diameter plastic optical fibers. Particularly in terms of experiments involving full-visible-spectrum-concentrated flux, quantitative research reports on the light leakage of optical fibers are very rare.

The purpose of this paper is to accurately measure the relationship between the relative transmittance of PMMA optical fibers and the incident angle in the visible-light band under the condition of natural light. This paper studies the light intensity distribution of the optical fiber output light cone at different incident angles, and draws the light distribution curve. The goal of this paper is to obtain a quantitative understanding of light leakage and to provide guidance for the optimization of PMMA optical fiber daylighting systems.

2. System Configuration

The evaluation of the optical fiber daylighting system for transmitting focused natural light is a complex task [46]. The optical fibers used in daylighting systems are utilized in a very different way than in communication systems. The former transmits a light cone covering the 400–700 nm band, while the latter transmits a single wavelength and parallel incidence laser light. Due to the serious angle effect of light leakage, the transmission efficiency analysis in optical fiber daylighting systems should not only consider the attenuation caused by the optical fiber length, but also pay attention to the light leakage effect. In

fiber optic communication systems, light travels along the fiber axis, and there is almost no light leakage, so its transmission attenuation is mainly considered by the fiber length. The nominal attenuation rate of plastic optical fibers is generally 180~200 dB/km, which is only applicable to a monochromatic light incident in parallel. In optical fiber daylighting systems, the attenuation rate of the plastic fibers is greater than this nominal value.

2.1. Platform

This experiment was performed on a two-axis turntable, as shown in Figure 1. An adjustable diaphragm, an infrared filter and heat-absorbing glass, and a Plano convex lens are fixed to the top of the turntable. By manually adjusting the azimuth and altitude angles, the turntable faces the sun, and the sunlight is focused on the entrance of the optical fiber. Table 1 shows the parameters of the experimental device.

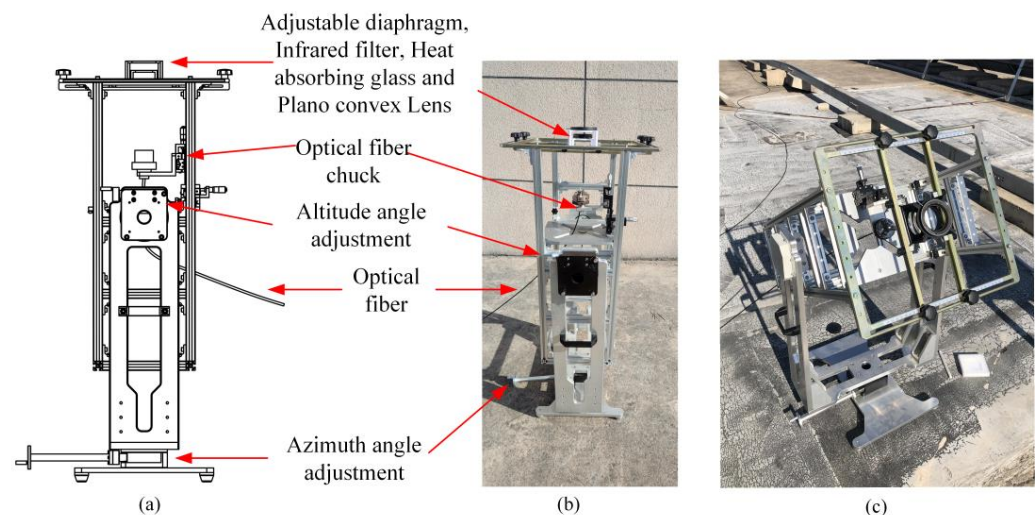


Figure 1. Two-axis turntable. (a) Three-dimensional structure of two-axis turntable. (b) Side view. (c) Picture of the two-axis turntable.

Table 1. Parameters of the experimental device.

Parameters	Units	Value
Lens aperture	mm	52
Focal length	mm	60
Optical fiber length	m	5, 10, 20
Range of the aperture of the diaphragm	mm	3–52
Critical angle of the fiber	degree	30
Core	-	PMMA
Cladding	-	Fluorinated polymer
Dichroic filter	-	Infrared interference filter
Type of absorbing glass	-	GRB3
Glass thickness	mm	2
Lens material	-	Glass
Model of the spectrometer	-	SPIC-300

The optical fiber is fixed on the chuck, as shown in Figure 2. By manually adjusting the knob, the optical fiber can be finely adjusted in three directions of X, Y, and Z. The precision of adjustment is 0.01 mm. The spot diameter is about 1 mm, so fine adjustment is necessary.

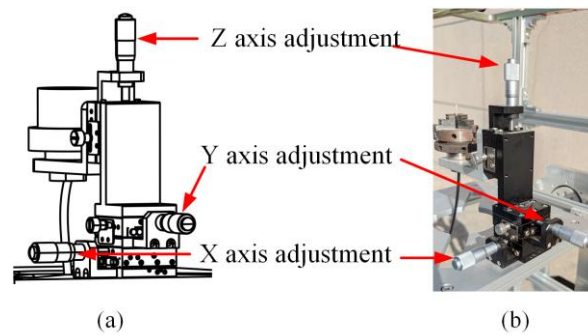


Figure 2. Optical fiber chuck. (a) Three-dimensional structure. (b) Picture of optical fiber chuck.

2.2. Plastic Optical Fibers

PMMA plastic optical fibers have the advantages of low price and good transparency. PMMA plastic optical fibers are made up of cores and claddings [47]. The fiber core has a greater refractive index than the cladding. Ideally, in the fiber core, incident light with an angle less than the critical angle can be transmitted as a total reflection [48]. The attenuation of optical fibers is only determined by the intrinsic absorption of the fiber core. In other words, ideally, incident light that satisfies the total reflection condition can be transmitted remotely. However, due to minor breakage at the core–cladding interface, light leakage occurs, resulting in lower optical transmission efficiency than the theoretical value. In particular, the larger the incident angle, the more serious the light leakage. Figure 3 shows the light path of the total reflection and light leakage within the fiber.

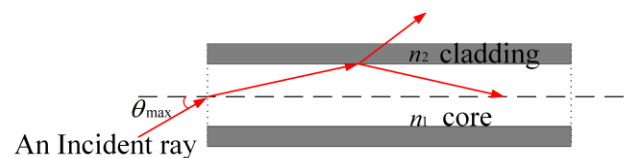


Figure 3. Light path of total reflection and light leakage.

In the fiber, when light is totally reflected, the maximum incident angle is called the critical angle, θ_{\max} . The critical angle is related to the numerical aperture (NA) [49]. NA is a critical parameter for describing the angular range of light received by the fiber [50]. The larger the value, the more light is collected. The relationship between the critical angle and the NA of the fiber is as follows [51]:

$$\theta_{\max} = \arcsin(NA) = \arcsin(\sqrt{n_1^2 - n_2^2}) \quad (1)$$

where θ_{\max} is the critical angle of the fiber, NA is the numerical aperture of the fiber, n_1 is the refractive index of the fiber core, and n_2 is the refractive index of the cladding. In this paper, θ_{\max} is 30° , and NA is 0.5, according to Equation (1).

2.3. Light Path Adjustment

Figure 4 shows that a bracket was printed for the installation of the diaphragm, the IR filter, the heat-absorbing glass, and the lens using 3D printing technology. Figure 5 shows the transmission of the concentrated sunlight. Such a light path structure not only realizes the continuous variation of different incident angles, but also effectively filters out infrared rays and prevents the PMMA optical fiber from being overheated and burnt so that the experiment can be carried out in a safe environment.

To achieve the quantitative measurement of light leakage, the optical fiber daylighting system needs to be equipped with an adjustable diaphragm. The available aperture of the diaphragm is 3–52 mm. Figure 6a,b show the variation of incident light as the diaphragm is changed from minimum to maximum. This study used a plano-convex lens to focus

sunlight. The focal length of the plano-convex lens is 60 mm. The relationship between the focal length and the incident angle is described as follows:

$$\theta = \arctan(D/2f) \quad (2)$$

where θ is the incident angle, f is the focal length, and D is the diaphragm effective diameter. From Equation (2), the variation of the incident angle ranges from 1.4° to 23.4° .

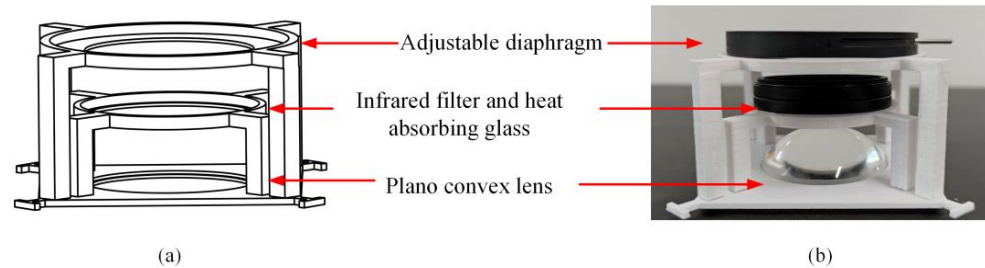


Figure 4. Bracket for installation of the diaphragm, IR filter, heat-absorbing glass, and lens. (a) Structure. (b) Front view.

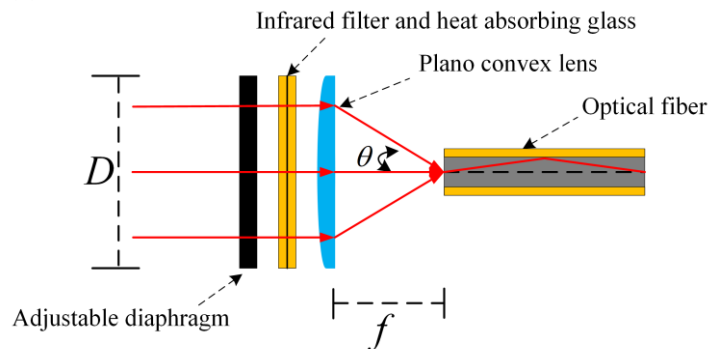


Figure 5. Schematic of the sunlight concentration and transmission via plastic optical fibers.

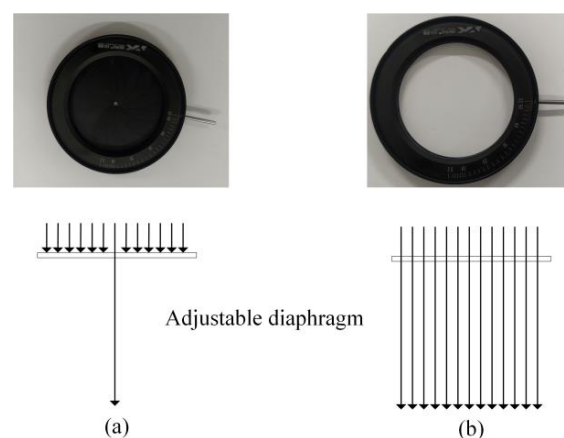


Figure 6. Variation of incident light with diaphragm diameter. (a) Minimum diaphragm diameter. (b) Maximum diaphragm diameter.

2.4. Filters

PMMA optical fibers are not resistant to high temperatures. Usually, PMMA optical fibers allow a working temperature within 70°C [52]. In the infrared band, PMMA fibers have a high absorption capacity [53]. The absorbed infrared (IR) light is converted into thermal energy, resulting in an increase in the temperature of the fibers. In the optical fiber daylighting system, sunlight is highly concentrated [54]. If not filtered, the PMMA optical fibers will overheat and melt, or even burn, due to the intense absorption of the infrared waves. Thus, in order to prevent the fiber from being burnt, this study uses a

hybrid filtering measure. First, this study used an IR interference filter. As shown in Figure 7a, IR interference filters can filter out 700–1200 nm infrared light while retaining 400–700 nm visible light. However, it cannot filter out infrared light exceeding 1200 nm, so further measures are required. In this study, heat-absorbing glass was used to filter infrared light at 1200–2500 nm. The heat-absorbing glass has a good filtering effect on infrared light at 1200–2500 nm, as shown in Figure 7b. The combination of an infrared filter and heat-absorbing glass affords a high transmission of visible light (400–700 nm) and filters out infrared light at 700–2500 nm, as shown in Figure 7c.

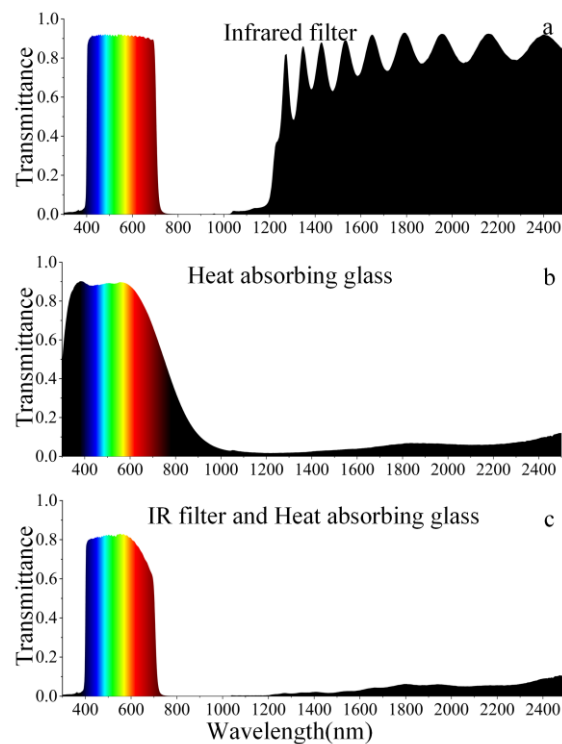


Figure 7. Transmittance of infrared filters and heat-absorbing glass. (a) IR filter. (b) Heat-absorbing glass. (c) Combination of infrared filter and heat-absorbing glass.

The experiment was carried out under the conditions of direct irradiation of $859 \pm 9 \text{ W/m}^2$ and an ambient temperature of $29 \text{ }^\circ\text{C}$. During the experiment, an infrared thermal imaging camera was used to observe the entrance of the PMMA fiber. During the whole experiment, the maximum recorded temperature of the optical fiber was $55.4 \text{ }^\circ\text{C}$, as shown in Figure 8. This shows that the filtering measure of the IR filter and the heat-absorbing glass can ensure the PMMA fiber works safely.

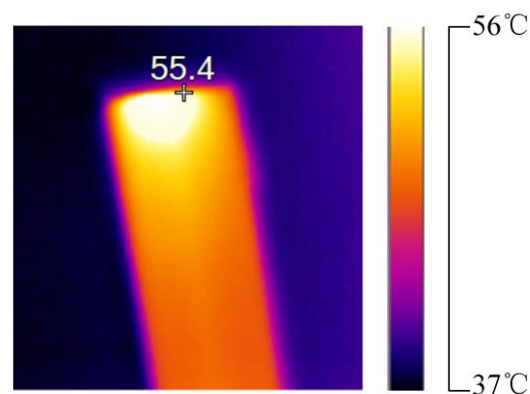


Figure 8. Infrared thermal image of the PMMA optical fiber under solar concentration (lens diameter is 52 mm, focal length is 60 mm, ambient temperature is $29 \text{ }^\circ\text{C}$, DNI is $859 \pm 9 \text{ W/m}^2$).

3. Experiments and Analysis

3.1. Experiments

The purpose of this study is to measure the dependence of the incident angle on relative transmittance. In order to facilitate a comparison, the study adopts normalization processing. In the experiment, PMMA optical fibers with different lengths are analyzed, namely 5 m, 10 m, and 20 m. The transmittance of fibers of 5 m, 10 m, and 20 m with the incident angle of 0 degrees is taken as the reference value. In the experiment, an integral sphere was adopted to measure the actual output luminous flux of PMMA. The data were normalized to obtain the relationship between the relative transmittance and the incident angle of the PMMA fibers.

From Figure 9, under ideal conditions, there is no light leakage. The ideal condition means that, without considering the small defects at the core–cladding interface, only the attenuation of the core is considered. Under the premise of satisfying total reflection, the theoretical transmission efficiency of the PMMA fibers only decreases slightly with the increase in the incident angle. However, the experiments show that the actual transmission efficiency does not match the prediction. Regardless of the length, when the incident angle is less than 13°, the relative transmission efficiency of the PMMA fibers is acceptable (greater than 50%). When the incident angle is greater than 13°, the relative transmission efficiency of the fiber drops rapidly. It can be predicted that when the incident angle reaches the critical angle of the PMMA fibers, the relative transmission efficiency will be close to zero. If a lens with an incident angle of 30 degrees is used to match the total reflection critical angle of the PMMA optical fiber, a large amount of light leakage will occur in the optical fiber photoconductive system. Therefore, if the global transmission efficiency of optical fiber daylighting systems is calculated by the nominal attenuation rate, an unacceptable deviation will occur.

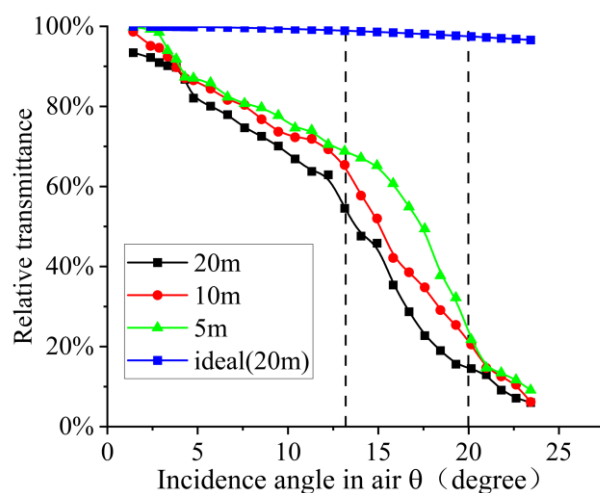


Figure 9. Comparison of real efficiency and theoretical efficiency of sunlight transmission via PMMA optical fibers.

Here, there is speculation that the light leakage is mainly due to the presence of small defects at the interface between the cladding and the fiber core, which destroys the total reflection conditions. Light leakage occurs when light encounters small defects. Light with an incident angle of 0 is transmitted parallel to the fiber axis, will not be reflected at the interface between the cladding and the fiber core, and will not be affected by interface defects, i.e., there is no light leakage. When the incident light is not parallel to the fiber axis, the light is reflected at the interface between the core and the cladding. When affected by interface defects, light leakage occurs with each reflection. Obviously, the larger the incident angle, the more light is reflected in the fiber and the more serious the light leakage. Due to the presence of light leakage, the reference value of the critical angle of the optical fiber in fiber optic daylighting systems is greatly weakened.

3.2. Spectrum

The pursuit of natural daylighting requires the high-fidelity transmission of visible light. In previous research, our team used liquid water to perform cooling and filtering [17]. The water cooling is not feasible in winter, so in this study, an air-cooling approach combining an infrared filter and heat-absorbing glass was developed. The spectrum of daylight covers a wide range, from 300 nm to 2500 nm, as shown in Figure 10a. The IR interference filter adopted is high transparency within 300–700 nm, shown in Figure 10b. From the figure, it is clear that the infrared interference filter can filter out the light of 700–1200 nm, and it does not work for spectrum larger than 1200 nm. In order to prevent the PMMA fiber from absorbing this part of the infrared light and causing the temperature to rise, this research also used the heat-absorbing glass to further filter the natural light. From Figure 10c, the heat-absorbing glass has a good absorption effect for infrared light greater than 1200 nm. Therefore, the study used a combination of an IR filter and heat-absorbing glass, which not only allows the visible light to be highly transmitted, but also filters the infrared light of 700–2500 nm, and its spectrum is shown in Figure 10d.

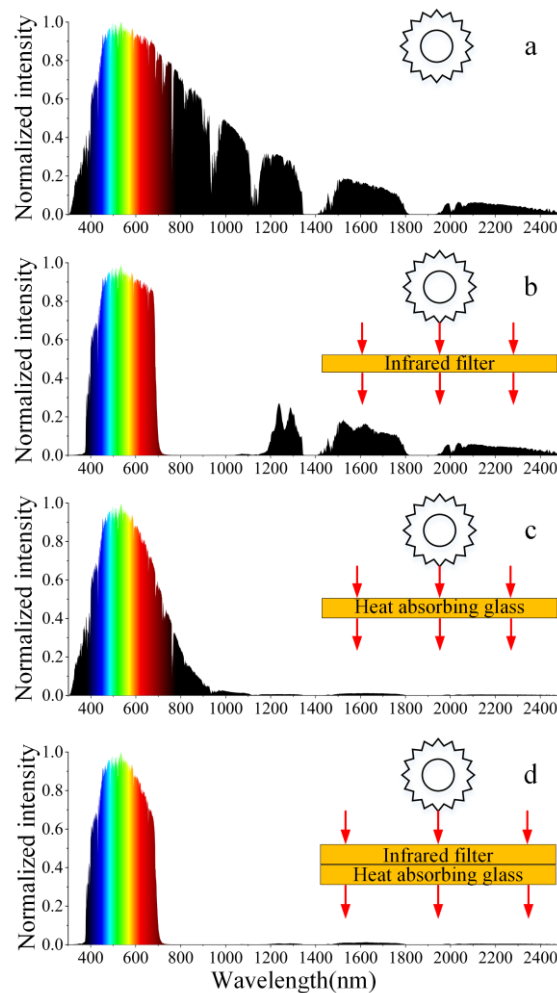


Figure 10. Sunlight spectrum and sunlight spectrum with different filtering measures. (a) Sunlight spectrum (AM1.5). (b) Output spectrum with an infrared filter. (c) Spectrum with heat-absorbing glass. (d) Sunlight spectrum filtered by IR filter and heat-absorbing glass.

In this study, a radiation spectrometer was used to measure the spectrum at the entrance of the PMMA optical fiber (Figure 11b). From this figure, in the visible light band of 400–780 nm, the output spectrum of the PMMA fiber is closer to that of natural light (Figure 11a). Therefore, although the daylighting system via PMMA fibers changes

the spectrum slightly, the quality of illumination is not decreased and can be used as an alternative to artificial lighting [55].

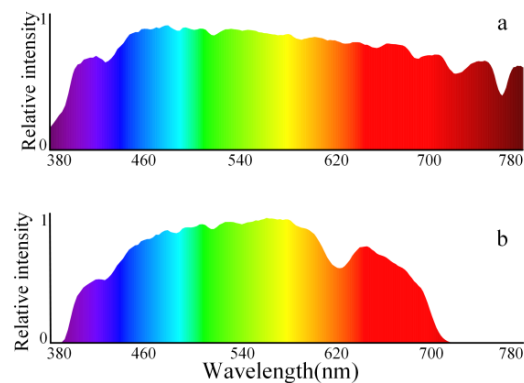


Figure 11. Spectral comparison of sunlight, output of PMMA fibers. (a) Sunlight. (b) PMMA fibers' output light.

3.3. Light Distribution

Quantitative measurements of the spatial distribution and luminous intensity of the light at the output of the PMMA fibers will facilitate the design of fiber optic daylighting systems [56]. In this study, a series of tests was carried out on a 20 m long fiber to study the optical properties of the light at the entrance of the fiber, which provided important reference information for the optimal allocation of daylighting systems.

Figures 12 and 13 show the 3D and 2D distributions of the light intensity in the area illuminated by the PMMA fiber, respectively. From the figure, the light intensity shows a symmetrical distribution with an intense center and darker edges. Figure 14 shows the relationship between the distribution and the angle of the illuminated work plane for different incident angles. This curve is the Candela light distribution curve [57]. Figure 14 shows that, under different incident angles, the angle of the output beam is less than $\pm 30^\circ$, which is equal to the critical angle of the PMMA fiber. This indicates that there is not only light leakage in the PMMA fibers, but also a change in the direction of light. Mode coupling occurs when different modes of light within a fiber interact and exchange energy, leading to changes in the direction of light propagation [58–60]. The reason for this change of light direction can be qualitatively analyzed from a physical point of view. There are two possible reasons for the change in light direction. One is that the defect at the interface between the fiber core and the cladding causes the direction of the reflected light to change, resulting in a change in the forward angle of the light. Another reason is the Rayleigh scattering effect produced by the polymer material molecules of the PMMA fiber. The Rayleigh effect scatters the forward light, which expands the angular range of the outgoing light at the fiber end.

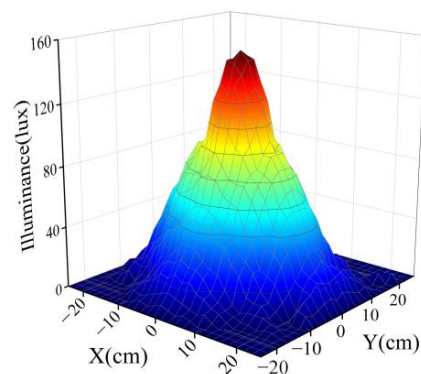


Figure 12. Three-dimensional distribution of the illumination distribution of a single 20 m long PMMA fiber (lens diameter is 52 mm, focal length is 60 mm, DNI is $859 \pm 9 \text{ W/m}^2$).

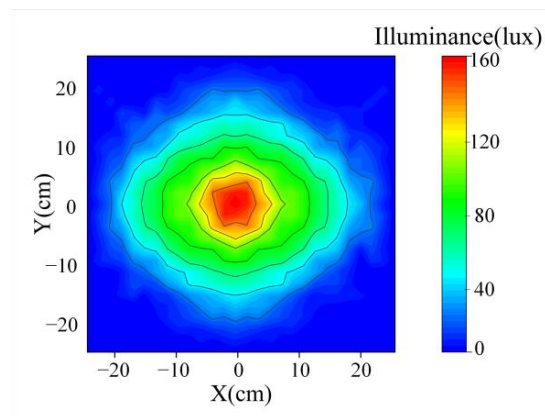


Figure 13. Two-dimensional distribution of the illumination distribution of a 20 m long PMMA fiber (lens diameter is 52 mm, focal length is 60 mm, DNI is $859 \pm 9 \text{ W/m}^2$).

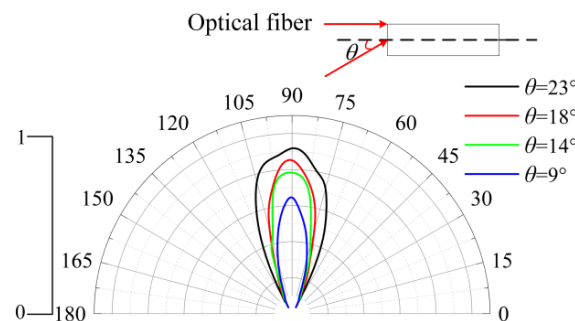


Figure 14. Light distribution curve of a 20 m long PMMA fiber at different incidence angles.

3.4. Analysis

The relation curve between light leakage and incident angle given in this study has certain guiding significance for the optical path optimization of optical fiber daylighting systems. That is, the incident angle of the condenser should not exceed 13 degrees. If the incident angle of the condenser is larger than this value, although the focused energy flux density is improved, the strong light leakage will lead to a decrease in the global transmission efficiency, which may not be worth the gain.

When light is transmitted in PMMA fibers, the absorption of the core causes light attenuation, while small defects at the core–cladding interface cause light leakage. In addition, PMMA material molecules produce Rayleigh scattering of light, causing light to scatter in all directions, resulting in light leakage. Figure 15 describes the attenuation process involved in light leakage in PMMA optical fibers. When the incident angle is greater than 25 degrees, the transmission efficiency is almost zero compared to that of zero-degree incident light. That is to say, although the critical angle of PMMA fiber with $\text{NA} = 0.5$ is 30 degrees, it is difficult to transmit daylight once the incident angle exceeds 25 degrees. Therefore, it is suggested that the incident angle effect of the actual transmission efficiency should be fully considered when selecting the angle of the lens cone in the design of the daylighting system using plastic optical fibers.

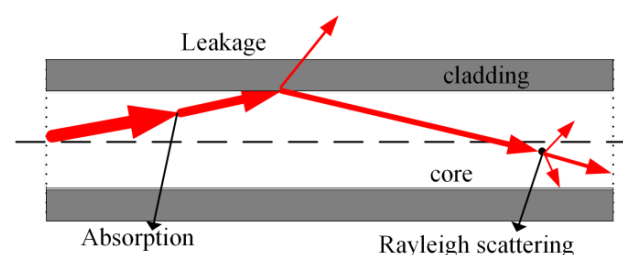


Figure 15. Light leakage processes in PMMA optical fibers.

Inspired by the experimental results, this study developed a PMMA fiber optic daylighting system with an incident angle of 13° , as shown in Figure 16. Table 2a shows a fiber daylighting system based on the parallel mechanism [61], with an incident angle of 24° and a global transmission efficiency of 13% (20 m). Table 2b shows a daylighting system using large Fresnel lens [62], with an incident angle of 18° and a global transmission efficiency of 15% (20 m). In Table 2c, the global transmission efficiency of the system is 18% (20 m), which is an improvement in efficiency compared with the previously developed systems by our team. By comparison, it can be obtained that the daylighting system has the highest efficiency when the incident angle is 13° , which is consistent with the experimental results in this paper.

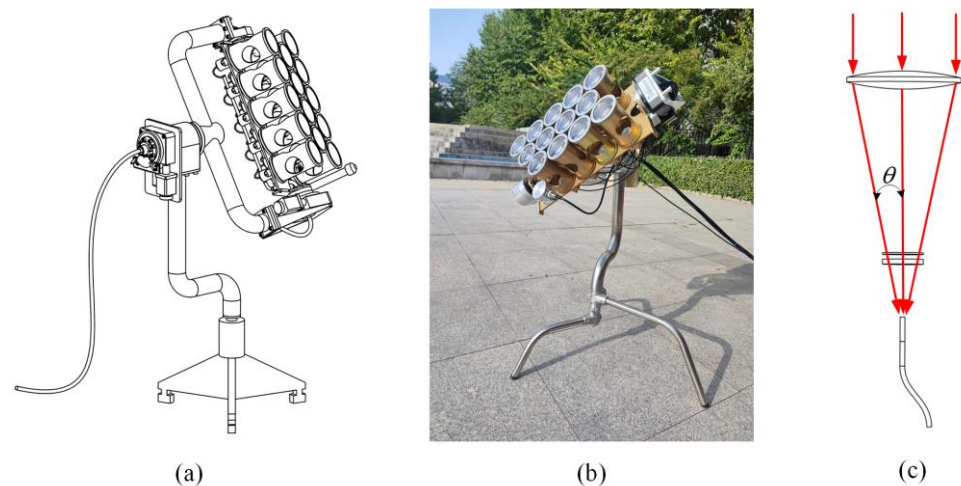


Figure 16. Developed daylighting system in this research. (a) Structure. (b) Picture. (c) Schematic of the sunlight concentration and transmission.

Table 2. Comparison of the three daylighting systems.

Picture	a	b	c
Lens aperture	100 mm	240 mm	70 mm
Focal length	110 mm	360 mm	150 mm
Incident angle	24°	18°	13°
Global efficiency	13% (20 m)	15% (20 m)	18% (20 m)
Input power	490 W/m^2	921 W/m^2	50 W/m^2
Output power	63 W/m^2	138 W/m^2	9 W/m^2

4. Conclusions

In this study, the light leakage phenomenon in PMMA fiber optic daylighting systems was quantitatively measured and analyzed. In the developed experimental platform, adjustable diaphragms were used to adjust the focusing beam angle. The relative transmission efficiency of 5 m, 10 m, and 20 m PMMA fibers for different incident lights was measured. The results show that the incident angle of light is negatively correlated with the relative transmission efficiency of PMMA optical fibers. When the incident angle is greater than 13° , the relative transmission efficiency decreases significantly, indicating that light leakage

occurs. As the incident angle increases, the number of reflections of light in the fiber increases, and the light leakage becomes more serious. When the incident angle reaches 25 degrees, the relative transmission efficiency of the fiber decreases to less than 10%. When the incident angle reaches a critical angle, which is 30°, the relative transmission efficiency is predicted to be close to 0. The experimental data illustrate that in the design of optical fiber daylighting systems, the nominal attenuation rate of the optical fiber is too ideal and not practical, and the leakage and the incident angle must be taken into account. Due to the influence of light leakage, the light distribution of the output of optical fiber daylighting systems also presents an uneven distribution of an intense center and darker edges, and the angle of the output beam is $\pm 30^\circ$. In the design of optical fiber daylighting systems, both the light leakage and the light distribution curve of the output beam should be considered.

Author Contributions: Methodology, Y.L. and J.S.; Data curation, L.Z., K.W. and H.W.; Writing—original draft, K.L.; Writing—review & editing, K.L. All authors have read and agreed to the published version of the manuscript.

Funding: This research was funded by The National Natural Science Foundation of China, grant number 52090064.

Institutional Review Board Statement: Not applicable.

Informed Consent Statement: Not applicable.

Data Availability Statement: Not applicable.

Acknowledgments: This work is supported by the Major Program of the National Natural Science Foundation of China (No. 52090064), partly supported by the Interdisciplinary Innovation Program of North China Electric Power University.

Conflicts of Interest: The authors have declared no conflict of interest.

References

1. Hollands, J.; Sesto, E.; Korjenic, A. Thermal Comfort in a Greened Office Building: Investigation and Evaluation through Measurement and Survey. *Sustainability* **2022**, *14*, 14450. [[CrossRef](#)]
2. Sun, J.; Li, Z.; Xiao, F.; Xiao, J. Generation of typical meteorological year for integrated climate based daylight modeling and building energy simulation. *Renew. Energy* **2020**, *160*, 721–729. [[CrossRef](#)]
3. Munaaim, M.A.C.; Al-Obaidi, K.M.; Ismail, M.R.; Rahman, A.M. Empirical Evaluation of the Effect of Heat Gain from Fiber Optic Daylighting System on Tropical Building Interiors. *Sustainability* **2014**, *6*, 9231–9243. [[CrossRef](#)]
4. Wong, L.I. A review of daylighting design and implementation in buildings. *Renew. Sustain. Energy Rev.* **2017**, *74*, 959–968. [[CrossRef](#)]
5. Vu, N.H.; Pham, T.T.; Shin, S. Modified optical fiber daylighting system with sunlight transportation in free space. *Opt. Express* **2016**, *24*, A1528–A1545. [[CrossRef](#)]
6. Yin, P.; Lv, J.; Wang, X.; Huang, R. A spectral splitting planar solar concentrator with a linear compound parabolic lightguide for optical fiber daylighting. *Renew. Energy* **2021**, *179*, 778–787. [[CrossRef](#)]
7. Ravn, M.; Mach, G.; Hansen, E.K.; Triantafyllidis, G. Simulating Physiological Potentials of Daylight Variables in Lighting Design. *Sustainability* **2022**, *14*, 881. [[CrossRef](#)]
8. Whang, A.J.W.; Yang, T.H.; Deng, Z.H.; Chen, Y.Y.; Tseng, W.C.; Chou, C.H. A Review of Daylighting System: For Prototype Systems Performance and Development. *Energies* **2019**, *12*, 2863. [[CrossRef](#)]
9. Schlegel, G.O.; Burkholder, F.W.; Klein, S.A.; Beckman, W.A.; Wood, B.D.; Muhs, J.D. Analysis of a full spectrum hybrid lighting system. *Sol. Energy* **2004**, *76*, 359–368. [[CrossRef](#)]
10. Sabbagh, M.; Mandourah, S.; Hareri, R. Light Shelves Optimization for Daylight Improvement in Typical Public Classrooms in Saudi Arabia. *Sustainability* **2022**, *14*, 13297. [[CrossRef](#)]
11. Xue, Y.; Liu, W. A Study on Parametric Design Method for Optimization of Daylight in Commercial Building's Atrium in Cold Regions. *Sustainability* **2022**, *14*, 7667. [[CrossRef](#)]
12. Casquero-Modrego, N. Optical fiber light scattering outdoor tests for interior daylighting. *Energy Build.* **2019**, *198*, 138–148. [[CrossRef](#)]
13. Gomes, M.G.; Santos, A.J.; Calhau, M. Experimental study on the impact of double tilted Venetian blinds on indoor daylight conditions. *Build. Environ.* **2022**, *225*, 109675. [[CrossRef](#)]
14. Song, J.; Yang, Y.; Zhu, Y.; Jin, Z. A high precision tracking system based on a hybrid strategy designed for concentrated sunlight transmission via fibers. *Renew. Energy* **2013**, *57*, 12–19. [[CrossRef](#)]

15. Mayhoub, M.S.; Elqattan, A.A.; Algendy, A.S. Experimental investigation of dust accumulation effect on the performance of tubular daylight guidance systems. *Renew. Energy* **2021**, *169*, 726–737. [[CrossRef](#)]
16. Mayhoub, M.S.; Rabboh, E.H. Daylighting in shopping malls: Customer's perception, preference, and satisfaction. *Energy Build.* **2022**, *255*, 111691. [[CrossRef](#)]
17. Song, J.; Wu, Z.; Wang, J.; Zhang, K.; Wang, K.; Liu, K.; Duan, L.; Hou, H. Application of highly concentrated sunlight transmission and daylighting indoor via plastic optical fibers with comprehensive cooling approaches. *Renew. Energy* **2021**, *180*, 1391–1404. [[CrossRef](#)]
18. Kandilli, C.; Ulgen, K. Review and modelling the systems of transmission concentrated solar energy via optical fibres. *Renew. Sustain. Energy Rev.* **2009**, *13*, 67–84. [[CrossRef](#)]
19. Sreelakshmi, K.; Ramamurthy, K. Review on fibre-optic-based daylight enhancement systems in buildings. *Renew. Sustain. Energy Rev.* **2022**, *163*, 112514. [[CrossRef](#)]
20. Li, X.; Wei, Y.; Zhang, J.; Jin, P. Design and analysis of an active daylight harvesting system for building. *Renew. Energy* **2019**, *139*, 670–678. [[CrossRef](#)]
21. Kribus, A.; Zik, O.; Karni, J. Optical fibers and solar power generation. *Sol. Energy* **2000**, *68*, 405–416. [[CrossRef](#)]
22. Vu, N.-H.; Shin, S. Cost-effective optical fiber daylighting system using modified compound parabolic concentrators. *Sol. Energy* **2016**, *136*, 145–152. [[CrossRef](#)]
23. Oh, S.J.; Chun, W.; Riffat, S.B.; Jeon, Y.I.; Dutton, S.; Han, H.J. Computational analysis on the enhancement of daylight penetration into dimly lit spaces: Light tube vs. fiber optic dish concentrator. *Build. Environ.* **2013**, *59*, 261–274. [[CrossRef](#)]
24. Wang, G.; Chen, Z.; Hu, P.; Cheng, X. Design and optical analysis of the band-focus Fresnel lens solar concentrator. *Appl. Therm. Eng.* **2016**, *102*, 695–700. [[CrossRef](#)]
25. Vu, D.T.; Vu, H.; Shin, S.; Tien, T.Q.; Vu, N.H. New mechanism of a daylighting system using optical-fiber-less design for illumination in multi-storey building. *Sol. Energy* **2021**, *225*, 412–426. [[CrossRef](#)]
26. Qin, X.; Zhang, X.; Qi, S.; Han, H. Design of Solar Optical Fiber Lighting System for Enhanced Lighting in Highway Tunnel Threshold Zone: A Case Study of Huashuyan Tunnel in China. *Int. J. Photoenergy* **2015**, *2015*, 1–10. [[CrossRef](#)]
27. Vu, D.T.; Nghiem, V.T.; Tien, T.Q.; Hieu, N.M.; Minh, K.N.; Vu, H.; Shin, S.; Vu, N.H. Optimizing optical fiber daylighting system for indoor agriculture applications. *Sol. Energy* **2022**, *247*, 1–12. [[CrossRef](#)]
28. Rouag-Saffidine, D. Adoption of optical fibres or of optical light films in architecture. *Renew. Energy* **1996**, *8*, 202–205. [[CrossRef](#)]
29. Song, J.; Luo, G.; Li, L.; Tong, K.; Yang, Y.; Zhao, J. Application of heliostat in interior sunlight illumination for large buildings. *Renew. Energy* **2018**, *121*, 19–27. [[CrossRef](#)]
30. Wang, C.; Abdul-Rahman, H.; Rao, S.P. Daylighting can be fluorescent: Development of a fiber solar concentrator and test for its indoor illumination. *Energy Build.* **2010**, *42*, 717–727. [[CrossRef](#)]
31. Ullah, I.; Shin, S. Highly concentrated optical fiber-based daylighting systems for multi-floor office buildings. *Energy Build.* **2014**, *72*, 246–261. [[CrossRef](#)]
32. Lv, J.; Xu, X.; Yin, P. Design of leak-free sawtooth planar solar concentrator for daylighting system. *J. Clean. Prod.* **2020**, *266*, 121895. [[CrossRef](#)]
33. Barbón, A.; Pardellas, A.; Fernández-Rubiera, J.A.; Barbón, N. New daylight fluctuation control in an optical fiber-based daylighting system. *Build. Environ.* **2019**, *153*, 35–45. [[CrossRef](#)]
34. Li, L.; Wang, J.; Yang, Z.; Luo, G.; Tong, K.; Zhao, J.; Song, J. An optical fiber daylighting system with large Fresnel lens. *Energy Procedia* **2018**, *152*, 342–347. [[CrossRef](#)]
35. Sedki, L.; Maaroufi, M. Design of parabolic solar daylighting systems based on fiber optic wires: A new heat filtering device. *Energy Build.* **2017**, *152*, 434–441. [[CrossRef](#)]
36. Savović, S.; Kovacevic, M.; Bajic, J.; Stupar, D.; Djordjevich, A.; Zivanov, M.; Drljača, B.; Simovic, A.; Oh, K. Temperature Dependence of Mode Coupling in low-NA Plastic Optical Fibers. *J. Light. Technol.* **2015**, *33*, 89–94. [[CrossRef](#)]
37. Savović, S.; Djordjevich, A.; Rui, M.; Savović, I. Investigation of performance properties of plastic optical fibers employed as a part of a traffic light system. *Quantum Electron.* **2021**, *51*, 1026–1029. [[CrossRef](#)]
38. Han, H.; Tai Kim, J. Application of high-density daylight for indoor illumination. *Energy* **2010**, *35*, 2654–2666. [[CrossRef](#)]
39. Song, J.; Zhu, Y.; Tong, K.; Yang, Y.; Reyes-Belmonte, M.A. A note on the optic characteristics of daylighting system via PMMA fibers. *Sol. Energy* **2016**, *136*, 32–34. [[CrossRef](#)]
40. Cariou, J.; Martin, L.; Dugas, J. Concentrated Solar-Energy Transport by Optical Fibers. *Am. Ceram. Soc. Bull.* **1980**, *59*, 343.
41. Mildner, D.F.R.; Chen, H. The neutron transmission through a cylindrical guide tube. *J. Appl. Cryst.* **1994**, *27*, 316–325. [[CrossRef](#)]
42. Dawei, L.; Yuri, N.; Luis Fraser, M.; Monteiro, M.L.F.; Manuel, C.-P. 200-W solar energy delivery with optical fiber bundles. *Proc. SPIE* **2017**, *3139*, 217–224.
43. Nakamura, T.; Comaskey, B.; Bell, M. Development of Optical Components for Space-Based Solar Plant Lighting. *SAE Tech. Pap.* **2000**, *1*. [[CrossRef](#)]
44. Dugas, J.; Sotom, M.; Martin, L.; Cariou, J.M. Accurate characterization of the transmittivity of largediameter multimode optical fibers. *Appl. Opt.* **1987**, *26*, 4198–4208. [[CrossRef](#)] [[PubMed](#)]
45. Feuermann, D.; Gordon, J.M.; Huleihil, M. Light leakage in optical fibers: Experimental results, modeling and the consequences for solar concentrators. *Sol. Energy* **2002**, *72*, 195–204. [[CrossRef](#)]

46. Chen, X.; Zhang, X.; Du, J. The potential of circadian lighting in office buildings using a fibre optics daylighting system in Beijing. *Build. Environ.* **2020**, *182*, 107118. [[CrossRef](#)]
47. Su, X.; Zhang, L.; Liu, Z.; Luo, Y.; Lian, J.; Liang, P. Daylighting performance simulation and analysis of translucent concrete building envelopes. *Renew. Energy* **2020**, *154*, 754–766. [[CrossRef](#)]
48. He, K.; Chen, Z.; Zhong, S.; Qian, Y.; Liu, H.; Yin, J.; Zhou, B. A solar fiber daylighting system without tracking component. *Sol. Energy* **2019**, *194*, 461–470. [[CrossRef](#)]
49. Ullah, I.; Lv, H.; Whang, A.J.-W.; Su, Y. Analysis of a novel design of uniformly illumination for Fresnel lens-based optical fiber daylighting system. *Energy Build.* **2017**, *154*, 19–29. [[CrossRef](#)]
50. Goel, C.; Yoo, S. Hybrid daylight harvesting system using static ball lens concentrator and movable optical fiber. *Sol. Energy* **2021**, *216*, 121–132. [[CrossRef](#)]
51. Barbón, A.; Sánchez-Rodríguez, J.A.; Bayón, L.; Barbón, N. Development of a fiber daylighting system based on a small scale linear Fresnel reflector: Theoretical elements. *Appl. Energy* **2018**, *212*, 733–745. [[CrossRef](#)]
52. Song, J.; Luo, N.; Wang, W. Configuration of daylighting system via fibers and experiments of concentrated sunlight transmission. In Proceedings of the 2013 International Conference on Materials for Renewable Energy and Environment, Nanjing, China, 19–21 August 2013; pp. 128–132.
53. Ioannides, N.; Chunga, E.B.; Bachmatiuk, A.; Gonzalez-Martinez, I.G.; Trzebicka, B.; Adebimpe, D.B.; Kalymnios, D.; Rummeli, M.H. Approaches to mitigate polymer-core loss in plastic optical fibers: A review. *Mater. Res. Express* **2014**, *1*, 032002. [[CrossRef](#)]
54. Zazoum, B.; Hassan, M.E.; Jendoubi, A. Solar optical fiber daylighting system with an IR filter: Experimental and modeling studies. *Energy Rep.* **2020**, *6*, 903–908. [[CrossRef](#)]
55. Lv, Y.; Xia, L.; Li, M.; Wang, L.; Su, Y.; Yan, J. Techno-economic evaluation of an optical fiber based hybrid solar lighting system. *Energy Convers. Manag.* **2020**, *225*, 113399. [[CrossRef](#)]
56. Andersen, M. Validation of the performance of a new bidirectional video-goniophotometer. *Light. Res. Technol.* **2006**, *38*, 295–313. [[CrossRef](#)]
57. Han, H.J.; Riffat, S.B.; Lim, S.H.; Oh, S.J. Fiber optic solar lighting: Functional competitiveness and potential. *Sol. Energy* **2013**, *94*, 86–101. [[CrossRef](#)]
58. Snchez Montero, D.R.; Vzquez, C. Multimode graded-index optical fibers for next-generation broadband access. In *Current Developments in Optical Fiber Technology*; IntechOpen: Rijeka, Croatia, 2013; Chapter 4, pp. 73–121. [[CrossRef](#)]
59. Montero, D.S.; Vazquez, C. Analysis of the electric field propagation method: Theoretical model applied to perfluorinated graded-index polymer optical fiber links. *Opt. Lett.* **2011**, *36*, 4116–4118. [[CrossRef](#)]
60. Pinzon, P.J.; Montero, D.S.; Tapetado, A.; Vazquez, C. Dual-Wavelength Speckle-Based SI-POF Sensor for Cost-Effective Detection of Microvibrations. *IEEE J. Sel. Top. Quantum Electron.* **2017**, *23*, 217–222. [[CrossRef](#)]
61. Song, J.; Jin, Z.; Zhu, Y.; Zhou, Z.; Yang, Y. Development of a fiber daylighting system based on the parallel mechanism and direct focus detection. *Sol. Energy* **2015**, *115*, 484–493. [[CrossRef](#)]
62. Yang, Z.; Li, L.; Wang, J.; Wang, W.; Song, J. Realization of high flux daylighting via optical fibers using large Fresnel lens. *Sol. Energy* **2019**, *183*, 204–211. [[CrossRef](#)]

Disclaimer/Publisher’s Note: The statements, opinions and data contained in all publications are solely those of the individual author(s) and contributor(s) and not of MDPI and/or the editor(s). MDPI and/or the editor(s) disclaim responsibility for any injury to people or property resulting from any ideas, methods, instructions or products referred to in the content.